# AlN MEMS Resonator with High Quality Factor

Wenli Liu*, Jinchao Li*, Zeji Chen, Yinfang Zhu, Jinling Yang, and Fuhua Yang
Institute of Semiconductors, Chinese Academy of Sciences
Beijing, P. R. China
yfzhu@semi.ac.cn, and jlyang@semi.ac.cn

Wenli Liu*, Jinchao Li*, Zeji Chen, Yinfang Zhu, Jinling Yang, and Fuhua Yang
The Center of Materials Science and Optoelectronics Engineering, University of Chinese Academy of Sciences
Beijing, P. R. China

Wenli Liu*, Jinchao Li*, Zeji Chen, Yinfang Zhu, and Jinling Yang
The State Key Laboratory of Transducer Technology
Shanghai, P. R. China
*These authors contributed equally to this work

***Abstract*—This paper reports a novel design on the notched supports coupled to the end of tethers to enhance the quality factor (*Q* factor) of the Lamb wave Aluminum Nitride (AlN) micro-electro-mechanical systems (MEMS) resonators. The anchor loss was reduced with the optimal notched support. Compared with the conventional flat-edge resonators, the *Q* factors of the fabricated resonators were improved by 1.42 times and 1.20 times at frequencies of 664 MHz and 839 MHz, respectively. This proposed approach can be adapted to various piezoelectric resonators which suffered from severe anchor loss induced by conventional tether designs.**

***Keywords—MEMS; AlN resonator; quality factor; notched support; PML***

## I. INTRODUCTION

With miniaturization of electronic devices, micro-electro-mechanical systems (MEMS) resonators have a variety of applications in sensors and wireless communications[1, 2]. The piezoelectric resonators have drawn great attention for their low impedance and high electromechanical couplings [3]. However, the piezoelectric MEMS resonators possess low quality factor (*Q* factor), which limits their practical applications in low phase noise oscillators, high sensitivity sensors, and high-end filters. Therefore, it is highly desired to enhance their *Q* values.

The anchor loss dominates energy dissipation of the piezoelectric resonators. There are often two routines to minimize the anchor loss. One scheme is to optimize the resonant structure to reduce the displacement at the edge coupled to the tether, such as the biconvex or butterfly-shaped resonant structures [4, 5], which trap the energy into the resonator so that the extra dissipations can be greatly reduced. Nevertheless, this type of resonators is susceptible to fabrication tolerances.

Another effective method aims to reflect the energy propagation from the resonator. One scheme is to combine the frame structure with the phononic crystals to form a complete acoustic bandgap which covers the resonance frequency, hereby, the propagation of acoustic waves can be effectively hindered [6].

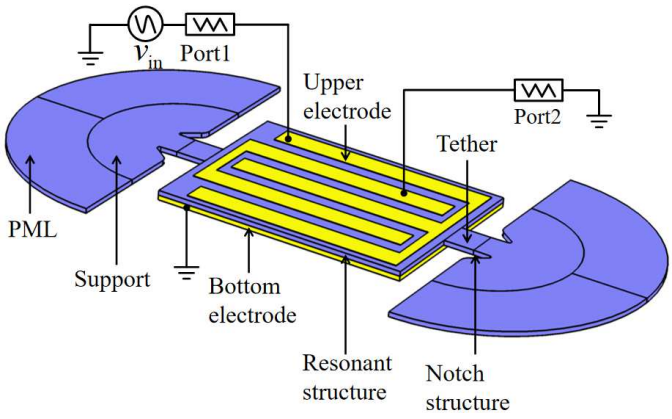


Fig. 1. Schematic diagram of the AlN resonator in this work

An alternative scheme is to introduce the acoustic reflector in substrate to produce the interfaces with mismatched acoustic impedances [7], thus a portion of acoustic waves can be reflected into the resonant structure. However, these additional structures will result in large footprint of the devices.

In this work, a novel design of notched support was demonstrated to reduce anchor loss of the resonators with compact resonator size.

## II. DESIGN AND FABRICATION

### A. Mode properties

As illustrated in Fig.1, the resonant structure is a rectangular thin-film plate. The two tethers couple the resonant structure and supports with two rounded triangle notches.

The upper electrode functions as uniformly distributed interdigital transducers (IDT). Adjacent electrodes are alternately used for driving and sensing so as to form a two-port configuration and reduce the feedthrough signal. The bottom electrode is grounded to enhance the electric field as well as suppress the parasitic capacitance. When ac driving signal is applied to the input electrode, the rectangular vibration based on

978-1-6654-3935-0/21/$31.00 ©2021 IEEE

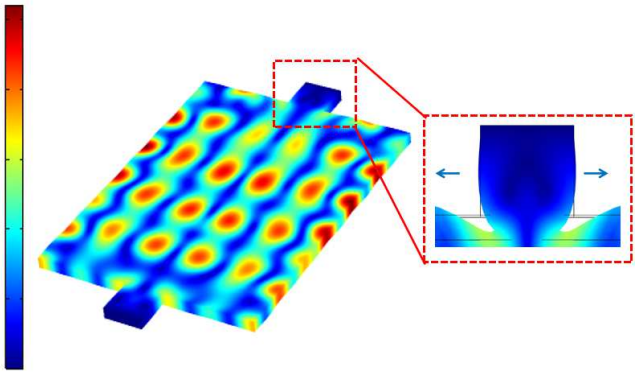

Fig. 2. The mode shape of resonator with notched support

the inverse piezoelectric effect, and the input signal is mechanically selected. Meanwhile, the charge generated by the mechanical vibrations accumulate at the output electrodes via the piezoelectric effect, the resonance peak can thus be extracted.

In-plane Lamb mode is adopted in this work to realize multiple resonant frequencies and $d_{31}$ piezoelectric coefficient is used for electromechanical coupling, that is, the piezoelectric film is driven into in-plane vibrations through the vertical electric field. In this work, with low loss and high electromechanical coupling coefficient, the 0th order symmetric mode ($S_0$) is selected for advantages of weak loss and high electromechanical couplings [8]. The mode shape in FEA simulation is depicted in Fig. 2. The resonance frequency of $S_0$ Lamb mode is described as[9]:

$$f = \frac{1}{2W_{\text{pitch}}}\sqrt{\frac{E}{\rho}} \tag{1}$$

where $E$ and $\rho$ represent Young's modulus and density of the AlN film. $W_{\text{pitch}}$ is the pitch width between the adjacent upper electrodes, and it is defined as:

$$W_{\text{pitch}} = \frac{W_{\text{pie}}}{n_{\text{IDT}}} \tag{2}$$

where $W_{\text{nie}}$ denotes the width of the thin plate and $n_{\text{IDT}}$ is the number of interdigital electrodes.

## B. Loss mechanisms

The energy loss sources of a resonator mainly include anchor loss, thermoelastic damping (TED), interface loss, air damping, and so on. $Q$ factor is expressed as [10]:

$$\frac{1}{Q_{\text{total}}} = \sum_i \frac{1}{Q_i} \tag{3}$$

where $Q_i$ is extracted from different loss mechanisms.

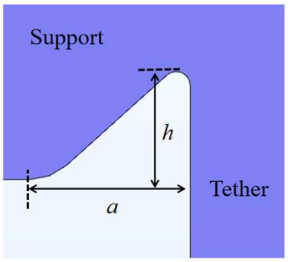


Fig. 3. Schematic of the notched support

Intrinsic loss is associated with the material properties and transduction mechanisms. For small in-plane displacement, Lamb wave resonators are insusceptible to air damping and TED [11]. Anchor loss is caused by acoustic waves leaking from the resonating body to the substrate through tethers. Anchor loss has been demonstrated as the prominent loss source for piezoelectric resonators [5, 7].

In the Lamb mode, the tethers and the resonant structure vibrate synchronously, the motions along the side direction are large. Therefore, in the case of flat-edge support, most of the acoustic energy radiates into supports. As shown in Fig. 1, the notches locate at the root of tether where it couples with the support, and solid-gas interface is formed between tether and support. Because of mismatched acoustic impedance between the tether and the support, more acoustic energy can be reflected to resonant structure.

## C. Optimized notched support design

A finite element analysis (FEA) model was established to optimize the notched support design. Perfectly Matched Layers (PML) were utilized to characterize the anchor loss of the resonator The acoustic wave transmission path in support is semicircular. As shown in Fig. 1, semicircular ring PMLs attached to the supports match the acoustic wavefront. To provide sufficient absorption of the acoustic waves radiating from any angle, the PML thickness is set as the resonant wavelength.

The Multiphysics of Piezoelectric Effect is utilized in simulation, and consequently the $Q$ factor is only related with anchor loss of the resonator. The simulated $Q$ factor related to the anchor loss can be calculated as [12]:

$$Q_{\text{anchor}} = \frac{\text{Re}(\omega_i)}{|2\,\text{Im}(\omega_i)|} \tag{4}$$

where $\text{Re}(\omega_i)$ and $\text{Im}(\omega_i)$ denote the real and imaginary parts of the angular resonance frequency. The imaginary part relates to energy loss of the FEA model.

The length of the triangle along the direction of the tether is defined as $h$, and the length at the side direction along tether is $a$ (shown as Fig. 3). The $Q_{\text{anchor}}$ values versus $h$ and $a$ are plotted in Fig. 4. The maximum $Q_{\text{anchor}}$ is 27 times the minimum $Q_{\text{anchor}}$. In this work, $h$ and $a$ were set as 5 μm and 6 μm to implement low anchor loss and retain the robustness of the device.

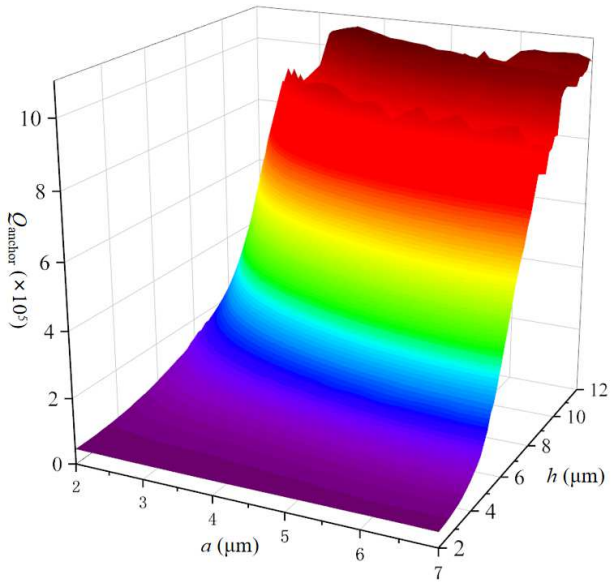


Fig. 4. Simulated relationship of $Q_{anchor}$ of 664MHz resonator versus $h$ and $a$

According to the principle of anchor loss, another effective method to optimize structural size is to analyze the displacement at of the tether-support attachment regions. However, compared with analyzing $Q_{anchor}$, since simulated frequency will change versus $h$ and $a$, it is an impractical work to gain a large amount of data to determine the geometry of notched supports.

The fabricated piezoelectric resonator is illustrated in Fig. 5. Aluminum Nitride (AlN) was used to build resonant structure. The upper and bottom electrodes is composed of Aluminum (Al) and Molybdenum (Mo), respectively. Finally, the resonator was released by etching Si in $XeF_2$ solution.

## III. RESULTS AND DISCUSSION

The SEM picture of fabricated resonator is shown in Fig. 6. The resonators were measured by Agilent E5071C network analyzer on a RF probe station. The spectra of notched and conventional resonators vibrating at 664 MHz and 839 MHz in air are displayed in Fig. 7 and Fig. 8, respectively. Compared with the conventional flat-edge resonators, the $Q$ factor of notched support design improves from 1060 to1510 (by 1.42 times) at 664 MHz, and from 1680 to 2030 (by 1.20 times) at 839 MHz.

At high frequency, the intrinsic loss tends to be more significant. Therefore, the $Q$ enhancement of the notched support design at 839 MHz is smaller than that at 664 MHz.

For RF devices, the motional impendence is a key parameter to integrate with circuit and the motional impendence of resonator can be calculated from the spectrum [13]:

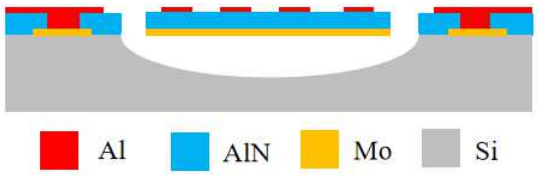


Fig. 5. Schematic of the fabricated piezoelectric resonators

$$R_m = 2Z_0(10^{-(\frac{G_{peak}}{20})} - 1) \tag{5}$$

where $Z_0$ is characteristic impedance and $G_{peak}$ is transmission gain at resonant peak. In terms of (5), the motional impendence decreases from 25.1 kΩ to 12.5 kΩ at 664 MHz, and from 3.1 kΩ to 2.4 kΩ at 839 MHz. The motional impendence of piezoelectric resonators is related to the $Q$ factor and $n_{IDT}$[14]:

$$R_{pie} \propto \frac{1}{n_{IDT} Q} \tag{6}$$

Pursuant to (6), the improvement of $Q$ factor and $n_{IDT}$ can achieve low motional impendence.

Essentially, the ideal notch design in the support can improve the resonator $Q$ values without mode distortions or spurious modes. However, as listed in TABLE I, due to the limited fabrication tolerance, there could be non-negligible divergence between the designed and actually fabricated sizes.

Table II compares the $Q$ enhancements among other reported resonators and this work's in terms of method, frequency, $Q$ enhancement, and $f \times Q$. The notched support structure is an effective and easy method to improve $Q$ factor. The $f \times Q$ product is limited by transduction mechanism and materials, and provides a reference of figure of merit (FOM) to compare resonators at different frequencies. The $f \times Q$ product of resonator in this work is comparable to those listed in TABLE II.

TABLE I. QUALITY FACTOR ENHANCEMENT TIMES

| *Frequency (MHz)* | *Simulated Q-improvement times* | *Measurement* | |
|---|---|---|---|
| | | *Q enhancement* | *times* |
| 664 | 1.45 | 1060→1510 | 1.42 |
| 839 | 1.28 | 1680→2030 | 1.20 |

TABLE II. COMPARISON ABOUT $Q$ ENHANCEMENT BETWEEN THE REPORTED RESONATORS AND THIS WORK

| *Reference* | *method* | *Frequency* (MHz) | *Q enhancement* (times) | *f×Q* (Hz) |
|---|---|---|---|---|
| 4 | Biconvex resonant structure | 70-141 | 5-11 | $1.46\times10^{12}$ |
| 5 | Butterfly-shaped resonant structure | ~863 | 1.42 | $4.11\times10^{12}$ |
| 6 | Both frame structure and phononic crystals | 51.75 | 7.80 | $2.45\times10^{11}$ |
| 7 | Acoustic reflectors | 27/110 | 1.25/5.60 | $1.32\times10^{12}$ |
| This wok | Notched supports | 664/839 | 1.42/1.20 | $1.70\times10^{12}$ |

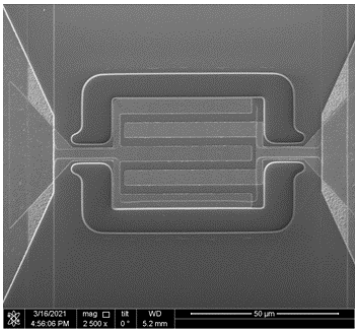

Fig. 6. SEM picture of notched-support resonator at 664 MHz

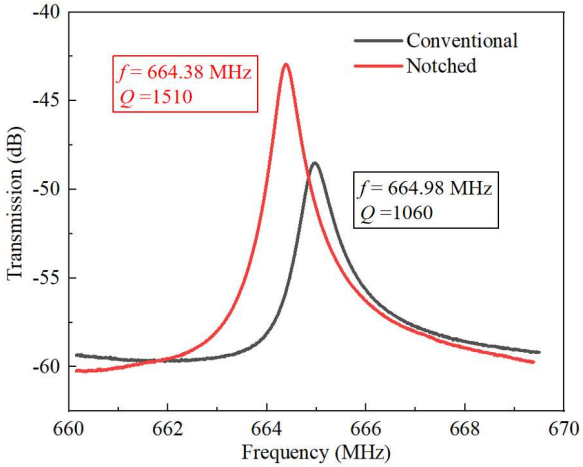


Fig. 7. Measured spectra of notched-support and conventional resonators at 664 MHz.

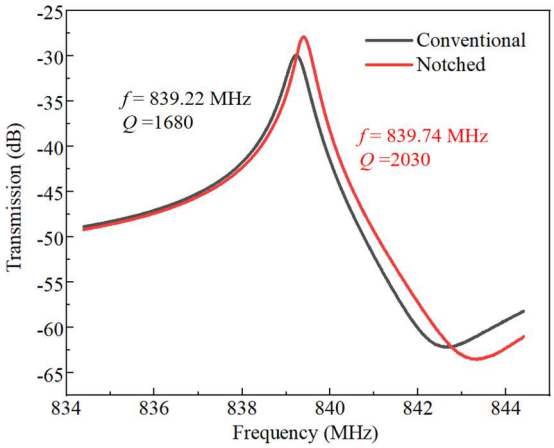


Fig. 8. Measured spectra of notched-support and conventional resonators at 839 MHz.

## IV. CONCLUSIONS

A novel design to reduce the anchor loss and to improve the *Q* factor of the AlN MEMS resonators is presented. The notched support coupled to the end of the tethers can suppress the propagation of acoustic waves into substrate. The *Q* factors of the fabricated resonators with frequencies of 664 MHz and 839 MHz were enhanced by 1.42 times and 1.20 times, respectively. The motional impendence reduces from 25.1 kΩ to 12.5 kΩ at 664 MHz, and from 3.1 kΩ to 2.4 kΩ at 839 MHz. The described methodologies can be widely adapted to resonators with enhanced *Q*, compact size, and higher reliability.

## ACKNOWLEDGMENT

This work was supported by the National Natural Science Foundation of China (61734007, 61804150, and 61874116), and the Youth Innovation Promotion Association of CAS (29E07RQC03).

## REFERENCES

[1] C. Zhao et al., "A review on coupled MEMS resonators for sensing applications utilizing mode localization," Sensors and Actuators A: Physical, vol. 249, pp. 93-111, 2016.

[2] J. Basu and T. K. Bhattacharyya, "Microelectromechanical resonators for radio frequency communication applications," Microsystem technologies, vol. 17, no. 10-11, p. 1557, 2011.

[3] B. Antkowiak, J. Gorman, M. Varghese, D. Carter, and A. Duwel, "Design of a high-Q, low-impedance, GHz-range piezoelectric MEMS resonator," in TRANSDUCERS'03. 12th International Conference on Solid-State Sensors, Actuators and Microsystems. Digest of Technical Papers (Cat. No. 03TH8664), 2003, vol. 1, pp. 841-846:

[4] C. Tu and J. E. Lee, "VHF-band biconvex AlN-on-silicon micromechanical resonators with enhanced quality factor and suppressed spurious modes," Journal of Micromechanics and Microengineering, vol. 26, no. 6, p. 065012, 2016.

[5] J. Zou, C.-M. Lin and A. P. Pisano, "Quality factor enhancement in Lamb wave resonators utilizing butterfly-shaped AlN plates," in 2014 IEEE International Ultrasonics Symposium, 2014, pp. 81-84.

[6] F.-H. Bao et al., "Quality factor improvement of piezoelectric MEMS resonator by the conjunction of frame structure and phononic crystals," Sensors and Actuators A: Physical, vol. 297, p. 111541, 2019.

[7] B. Harrington and R. Abdolvand, "In-plane acoustic reflectors for reducing effective anchor loss in lateral–extensional MEMS resonators," Journal of Micromechanics and Microengineering, vol. 21, no. 8, p. 085021, 2011.

[8] V. Yantchev and I. Katardjiev, "Thin film Lamb wave resonators in frequency control and sensing applications: a review," Journal of Micromechanics and Microengineering, vol. 23, no. 4, p. 043001, 2013.

[9] R. Abdolvand, H. Fatemi, and S. Moradian, "Quality factor and coupling in piezoelectric mems resonators," in Piezoelectric MEMS Resonators: Springer, 2017, pp. 133-152.

[10] G. Piazza, P. J. Stephanou and A. P. Pisano, "Piezoelectric aluminum nitride vibrating contour-mode MEMS resonators," Journal of Microelectromechanical systems, vol. 15, no. 6, pp. 1406-1418, 2006.

[11] R. N. Candler et al., "Investigation of energy loss mechanisms in micromechanical resonators," in TRANSDUCERS'03. 12th International Conference on Solid-State Sensors, Actuators and Microsystems. Digest of Technical Papers (Cat. No. 03TH8664), 2003, vol. 1, pp. 332-335:

[12] T. Koyama et al., "Simulation tools for damping in high frequency resonators," in SENSORS, 2005 IEEE, 2005, p. 4 pp.

[13] T. J. Cheng and S. A. Bhave, "High-Q, low impedance polysilicon resonators with 10 nm air gaps," in 2010 IEEE 23rd International Conference on Micro Electro Mechanical Systems (MEMS), 2010, pp. 695-698:

[14] J. Zou, High-performance aluminum nitride Lamb wave resonators for RF front-end technology. University of California, Berkeley, 2015.